京都大学学術情報リポジトリ
KURENAI 紅
Kyoto University Research Information Repository

京都大学
KYOTO UNIVERSITY

Title	Coordination and interface analysis of atomic-layer-deposition Al2O3 on Si(001) using energy-loss near-edge structures
Author(s)	Kimoto, K; Matsui, Y; Nabatame, T; Yasuda, T; Mizoguchi, T; Tanaka, I; Toriumi, A
Citation	APPLIED PHYSICS LETTERS (2003), 83(21): 4306-4308
Issue Date	2003-11-24
URL	http://hdl.handle.net/2433/39661
Right	Copyright 2003 American Institute of Physics. This article may be downloaded for personal use only. Any other use requires prior permission of the author and the American Institute of Physics.
Type	Journal Article
Textversion	none; publisher

Kyoto University

Coordination and interface analysis of atomic-layer-deposition Al_2O_3 on Si(001) using energy-loss near-edge structures

K. Kimoto[a)] and Y. Matsui
Advanced Materials Laboratory, National Institute for Materials Science (NIMS), 1-1 Namiki, Tsukuba, Ibaraki 305-0044, Japan

T. Nabatame
MIRAI Project, Association of Super-Advanced Electronics Technologies (ASET), 16-1 Onogawa, Tsukuba, Ibaraki 305-8569, Japan

T. Yasuda
MIRAI Project, Advanced Semiconductor Research Center, National Institute of Advanced Industrial Science and Technology (AIST), 16-1 Onogawa, Tsukuba, Ibaraki 305-8569, Japan

T. Mizoguchi and I. Tanaka
Department of Material Science & Engineering, Kyoto University, Sakyo-ku, Kyoto 606-8501, Japan

A. Toriumi
Department of Materials Science, Graduate School of Engineering, The University of Tokyo, 7-3-1 Hongo, Bunkyo-ku, Tokyo 113-8656, Japan, and MIRAI project, AIST, Japan.

(Received 3 March 2003; accepted 26 September 2003)

The coordination and interface of Al_2O_3 formed on Si(001) by atomic layer deposition (ALD) were studied using electron energy-loss spectroscopy in a transmission electron microscope. Al energy-loss near-edge structures (ELNESs) were interpreted using first-principles calculations. The Al L_{23} ELNESs show two peaks at 78.2 and 79.7 eV, which originate from tetrahedrally and octahedrally coordinated aluminum, respectively. The depth profile of coordination in ALD Al_2O_3/Si was investigated. While both tetrahedrally and octahedrally coordinated Al atoms exist in the ALD Al_2O_3, the former is dominant near the interface. Aluminum silicate was detected near the interface, and it may cause the difference in aluminum coordination. © *2003 American Institute of Physics.* [DOI: 10.1063/1.1629397]

The development of high dielectric constant (high-*k*) materials is one of the critical subjects for future complementary metal-oxide-semiconductor (CMOS) devices.[1] Al_2O_3 is a prospective high-*k* material as a replacement for SiO_2, because of its large band gap, and its thermal and chemical stability. The electrical properties of CMOS devices directly depend, not only on the Al_2O_3 film, but also on the interface between Al_2O_3 film and Si substrate. Therefore, the microstructure and crystallographic studies of amorphous Al_2O_3 film are required, such as the determination of the Al coordination and its depth profile with high-spatial resolution. Al_2O_3 ultrathin films on Si substrates have been analyzed using x-ray photoelectron spectroscopy,[2] secondary ion mass spectrometry,[3] and other methods.[3–5]

We applied electron energy-loss spectroscopy (EELS) in a transmission electron microscope (TEM),[6] which is effective for the characterization of ultrathin dielectrics for CMOS devices in terms of high spatial resolution.[7–9] Energy-loss near-edge structure (ELNES) in an EEL spectrum is sensitive to the valence and the coordination of specific elements.[10,11] In the present study, the Al coordination and interface of Al_2O_3/Si are investigated using TEM EELS and the first-principles calculations of ELNES.

An Al_2O_3/Si specimen was prepared by atomic layer deposition (ALD) of a 5-nm-thick layer at 300 °C using $Al(CH_3)_3$ and H_2O precursors on a H-terminated Si(001) wafer.[12] The ALD process is gaining acceptance because it allows controllable and uniform deposition with an accuracy of an atomic layer. Rapid thermal annealing (RTA) was done after the deposition in a mixture of Ar+1% O_2 at 750 °C. A TEM specimen for cross-sectional observations was made by mechanical thinning and ion milling. We also analyzed a few γ-alumina specimens for ELNES interpretation: commercial γ-alumina powder (Nilaco Co., 99.99%) and ultrafine γ-alumina particles prepared by the direct oxidation of aluminum in a mixture of Ar and O_2.[13] Contrary to Si coordination in silica, the Al atom can occupy both tetrahedrally and octahedrally coordinated sites in transition aluminas, such as γ-alumina. The γ-alumina (widely defined) includes γ (narrowly defined), η, θ, and other structures. These γ-alumina structures are basically defective spinel structures with cation-site vacancies. The proportion of Al coordination (tetrahedral:octahedral) is reported as follows: 36:51 (η), 32:68 (γ), and 50:50 (θ);[14] however, there is still a controversy about cation-site vacancies.[15] Although the proportions of Al coordination in the present specimens (commercial powder and ultrafine particles) are not clear, they include both tetrahedrally and octahedrally coordinated Al atoms.

A TEM (Hitachi, HF-3000) with an energy-loss spectrometer (Gatan, GIF2002) was used at an acceleration voltage of 300 kV. Due to the field-emission electron gun of the

a)Author to whom correspondence should be addressed; electronic mail: kimoto.koji@nims.go.jp

 © 2003 American Institute of Physics
Downloaded 30 May 2007 to 130.54.110.22. Redistribution subject to AIP license or copyright, see http://apl.aip.org/apl/copyright.jsp

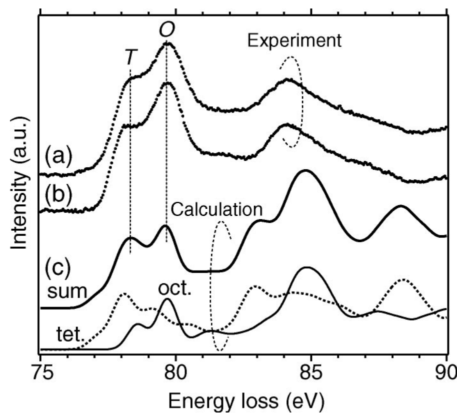

FIG. 1. Experimental and calculation results of Al L_{23} ELNES. Two experimental results obtained using commercial γ-Al_2O_3 powder (a) and ultrafine γ-Al_2O_3 particles prepared by the direct oxidation of aluminum (b) are shown. Calculation results are shown as the sum (sum) of two calculations, in which tet. and oct. Al sites are excited.

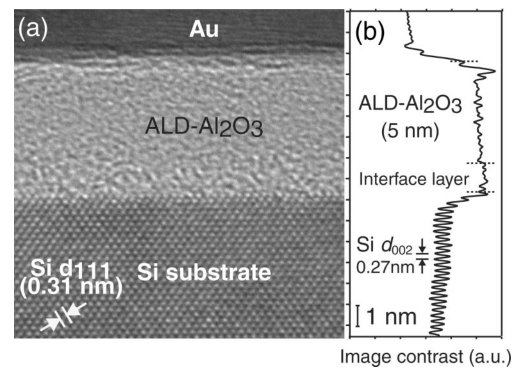

FIG. 2. Cross-sectional TEM image of ALD Al_2O_3/Si (a) and the profile of the TEM image contrast (b).

TEM and a customized software for drift correction, a high energy resolution of about 0.3 eV was realized in EELS.[16] Al L_{23} and Si L_{23} ELNESs were recorded. We also applied a spatially resolved technique to analyze the thin film specimen. By this technique, EEL spectra from the different positions were measured simultaneously using a two-dimensional detector. The details in the spatially resolved EELS techniques have been reported elsewhere.[9,17]

Theoretical calculations of Al L_{23} ELNES were made using the density-functional-theory-based first-principles orthogonalized linear combinations of atomic orbitals (OLCAO) method.[15,18] In the present study, the crystal structure of θ-Al_2O_3[14] was used for the OLCAO calculations. We prepared two supercells composed of 80 atoms, in which the Al site of interest is located at the center. Since fine structures in an EEL spectrum depend mainly on the neighboring atoms, the calculation results of crystalline Al_2O_3 are applicable for interpreting ELNESs of amorphous Al_2O_3. It is known that ''core-hole effect'' should be implemented for the first-principles calculation of ELNESs,[19–21] because the final state is drastically different from the ground state, owing to the interaction between the electron and the core hole. The present first-principles calculations with the core-hole effect can reproduce experimental ELNESs, such as so-called ''exciton peaks'' observed near the threshold. Here, the core-hole effect has been implemented in the OLCAO method as reported by Mo *et al.*[21] The initial ground state and the final state with a core-hole at the center Al site were calculated, and the photo absorption cross section was obtained by calculating the dipole transition matrix. Absolute transition energy (energy-loss) was evaluated as the difference in total energies in the initial and the final state. The ELNES calculation results of the OLCAO method have already shown good agreement for silicon nitride[11] and a few oxides.[21,22]

Figures 1(a) and 1(b) show the experimental results of Al L_{23} ELNESs for two γ-aluminas: (a) the commercial powder and (b) the ultrafine particles. The Al L_{23} ELNES has two peaks at 78.2 and 79.7 eV, as indicated by T and O. The two spectra look similar, but the intensity ratio of peaks T to O is slightly different. To identify the origin of the two peaks T and O, we calculated two ELNESs in which the excited Al site is set at a tetrahedral site (tet.) or octahedral site (oct.) [Fig. 1(c)]. In the experiment, both tetrahedral and octahedral sites are equally excited independently, so the two calculation results (tet. and oct.) are simply summed as the calculation result (sum) for comparison with experimental results. Calculations successfully reproduce the experimental ELNES, including absolute energy loss of the two peaks. Few pioneering studies on Al ELNES calculation exist,[23,24] and our calculation quantitatively shows that peak T at about 78.2 eV mainly originated from the tetrahedrally coordinated Al and peak O at about 79.7 eV from the octahedrally coordinated one. These assignments are informative to interpret various ELNESs of related materials, such as $HfAlO_x$. The aforementioned difference in the experimental peak ratio (T:O) is considered to be due to the difference in the proportion of Al coordination (tetrahedral:octahedral), and is consistent with the variation of its proportion in several γ-aluminas.[14]

Figure 2(a) shows cross-sectional TEM image of ALD Al_2O_3/Si specimen, indicating an amorphous ALD Al_2O_3 layer. The line profile of the TEM image contrast [Fig. 2(b)] shows that image brightness is relatively high near the interface, suggesting an interface layer. We estimated the interface layer to be roughly 1.3 nm thick. Figure 3 shows

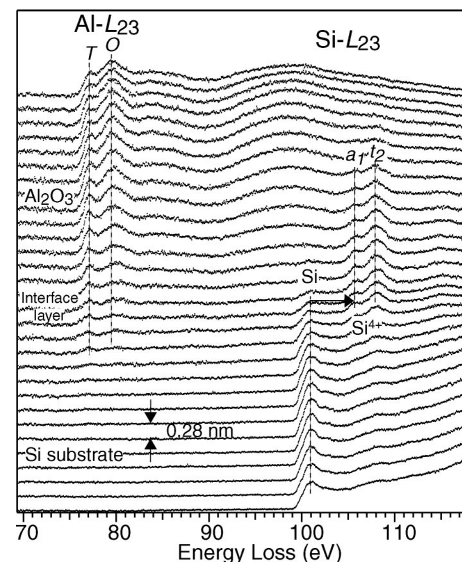

FIG. 3. Spatially resolved EEL spectra indicating Al L_{23} and Si L_{23} ELNESs. Note the depth dependence of peak intensity ratio (T:O) in Al L_{23}, and the chemical shift of Si L_{23} near the interface. The interval of each EEL spectrum is 0.28 nm in depth.

Downloaded 30 May 2007 to 130.54.110.22. Redistribution subject to AIP license or copyright, see http://apl.aip.org/apl/copyright.jsp

spatially-resolved EEL spectra obtained across a region from the Si substrate to the ALD Al_2O_3 layer. The background in each EEL spectrum was subtracted using the power-low model.[6] The interval of each spectrum is 0.28 nm in depth. We discuss the Al L_{23} ELNES and its depth profile. The aforementioned peaks T and O are also observed in the ALD Al_2O_3. One specific feature is that peak O is high on the upper side of Al_2O_3 layer and peak T is relatively intense near the Si substrate. Peak T near the interface is extraordinarily high compared to γ-aluminas. It is known that thermal treatment eventually transforms amorphous Al_2O_3 to γ-alumina,[14] but under insufficient thermal treatment such as the present RTA, tetrahedrally coordinated Al is dominant, especially near the interface.

We studied the interface layer in terms of Si chemical bonding based on Si L_{23} ELNES (Fig. 3). In the Si substrate, the Si L_{23} edge is at 100 eV for the midpoint of edge onset, and is chemically shifted near the interface by about 5 eV, which is the same as observed in silicates containing SiO_4 tetrahedra[6] or in amorphous SiO_2.[9,17] Although peak intensities gradually decrease toward the upper side, the Si L_{23} fine structure does not differ in the amorphous layer. We thus conclude that an aluminum silicate interface layer is formed, and Si atoms exist as SiO_4 tetrahedra. It is estimated that aluminum silicate near the interface may cause the difference in aluminum coordination, because tetrahedrally coordinated cation is dominant in silica. The aluminum silicate layer is considered to be grown by the Si oxidation during the ALD process, therefore this should be minimized to optimize the growth conditions.[12]

We thank Dr. Kusunoki of Japan Fine Ceramics Center for providing the ultrafine particles and Prof. W. Y. Ching of the University of Missouri for allowing us to use the OLCAO code. This work was supported by the NEDO/MIRAI project. We are also grateful for support from Nanotechnology Support Project by MEXT of Japan.

[1] G. D. Wilk, R. M. Wallace, and J. M. Anthony, J. Appl. Phys. **89**, 5243 (2001).
[2] R. Reiche, F. Yubero, J. P. Espinós, and A. R. González-Elipe, Surf. Sci. **457**, 199 (2000).
[3] L. G. Gosset, J.-F. Damlencourt, O. Renault, D. Rouchon, P. Holliger, A. Ermolieff, I. Trimaille, J.-J. Ganem, F. Martin, and M.-N. Séméria, J. Non-Cryst. Solids **303**, 17 (2002).
[4] M. Copel, E. Cartier, E. P. Gusev, S. Guha, N. Bojarczuk, and M. Poppeller, Appl. Phys. Lett. **78**, 2670 (2001).
[5] T. M. Klein, D. Niu, W. S. Epling, W. Li, D. M. Maher, C. C. Hobbs, R. I. Hegde, I. J. R. Baumvol, and G. N. Parsons, Appl. Phys. Lett. **75**, 4001 (1999).
[6] R. F. Egerton, *Electron Energy-Loss Spectroscopy in the Electron Microscope*, 2nd ed. (Plenum, New York, 1996).
[7] P. E. Batson, Nature (London) **366**, 727 (1993).
[8] D. A. Muller, T. Sorsch, S. Moccio, F. H. Baumann, K. Evans-Lutterodt, and G. Timp, Nature (London) **399**, 758 (1999).
[9] K. Kimoto, K. Kobayashi, T. Aoyama, and Y. Mitsui, Micron **30**, 121 (1999).
[10] F. Hofer, in *Energy-Filtering Transmission Electron Microscopy*, edited by L. Reimer (Springer, New York, 1995), p. 225.
[11] I. Tanaka, T. Mizoguchi, T. Sekine, H. He, K. Kimoto, T. Kobayashi, S.-D. Mo, and W. Y. Ching, Appl. Phys. Lett. **78**, 2134 (2001).
[12] R. Kuse, N. Miyata, M. Kundu, T. Yasuda, K. Iwamoto, K. Kimoto, T. Nabatame, and A. Toriumi, *Extended Abstracts of the 2002 International Conference SSDM* (JSAP), Nagoya, Japan, 2002, p. 454.
[13] M. Kusunoki, M. Rokkaku, Y. Ikuhara, and H. Yanagida, Mater. Trans., JIM **39**, 110 (1998).
[14] R.-S. Zhou and R. L. Snyder, Acta Crystallogr., Sect. B: Struct. Sci. **47**, 617 (1991).
[15] S.-D. Mo, Y.-N. Xu, and W.-Y. Ching, J. Am. Ceram. Soc. **80**, 1193 (1997).
[16] K. Kimoto and Y. Matsui, J. Microsc. **208**, 224 (2002).
[17] K. Kimoto, T. Sekiguchi, and T. Aoyama, J. Electron Microsc. **46**, 369 (1997).
[18] S.-D. Mo and W. Y. Ching, Phys. Rev. B **57**, 15219 (1998).
[19] T. Lindner, H. Sauer, W. Engel, and K. Kambe, Phys. Rev. B **33**, 22 (1986).
[20] K. Lie, R. Brydson, and H. Davock, Phys. Rev. B **59**, 5361 (1999).
[21] S.-D. Mo and W. Y. Ching, Phys. Rev. B **62**, 7901 (2000).
[22] K. Kimoto, K. Ishizuka, T. Mizoguchi, I. Tanaka, and Y. Matsui, J. Electron Microsc. **52**, 299 (2003).
[23] R. Brydson, H. Müllejans, J. Bruley, P. A. Trusty, X. Sun, J. A. Yeomans, and M. Rühle, J. Microsc. **177**, 369 (1995).
[24] P. L. Hansen, R. Brydson, D. W. McComb, and I. Richardson, Microsc. Microanal. Microstruct. **5**, 173 (1994).

Downloaded 30 May 2007 to 130.54.110.22. Redistribution subject to AIP license or copyright, see http://apl.aip.org/apl/copyright.jsp